Estimating the effect of tree uprooting on variation of soil horizon depth by confronting pedogenetic simulations to measurements in a Belgian loess area

P. A. Finke,[1] T. Vanwalleghem,[2] E. Opolot,[1] J. Poesen,[3] and J. Deckers[3]

Received 16 April 2013; revised 23 September 2013; accepted 25 September 2013; published 15 October 2013.

[1] Spatial patterns of soil often do not reflect those of topographic controls. We attempted to identify possible causes of this by comparing observed and simulated soil horizon depths. Observed depths of E, Bt, BC, C1, and C2 horizons in loess-derived soils in Belgium showed a weak to absent relation to terrain attributes in a sloping area. We applied the soil genesis model SoilGen2.16 onto 108 1 × 1 m^2 locations in a 1329 ha area to find possible causes. Two scenarios were simulated. Model 1 simulated soil development under undisturbed conditions, taking slope, aspect, and loess thickness as the only sources of variations. Model 2 additionally included a stochastic submodel to generate tree-uprooting events based on the exposure of trees to the wind. Outputs of both models were converted to depths of transitions between horizons, using an algorithm calibrated to horizon depths observed in the field. Model 1 showed strong correlations between terrain attributes and depths for all horizons, although surprisingly, regression kriging was not able to model all variations. Model 2 showed a weak to absent correlation for the upper horizons but still a strong correlation for the deeper horizons BC, C1, and C2. For the upper horizons the spatial variation strongly resembled that of the measurements. This is a strong indication that bioturbation in the course of soil formation due to treefalls influences spatial patterns of horizon depths.

Citation: Finke, P. A., T. Vanwalleghem, E. Opolot, J. Poesen, and J. Deckers (2013), Estimating the effect of tree uprooting on variation of soil horizon depth by confronting pedogenetic simulations to measurements in a Belgian loess area, *J. Geophys. Res. Earth Surf.*, *118*, 2124–2139, doi:10.1002/jgrf.20153.

1. Introduction

[2] The characterization and prediction of soil properties, such as depth, texture, or salinity, is crucial for many ecological, hydrological, geomorphic, or agronomic models [*Rantakari et al.*, 2012; *Finke and Bosma*, 1993; *Claessens et al.*, 2007; *Wallach et al.*, 2011]. In agricultural areas, especially on sloping terrain, soil redistribution by erosion has been shown to control the spatial distribution of soil properties like horizon depth, texture, stoniness, or soil organic carbon [*Poesen et al.*, 1997; *Li and Lindstrom*, 2001; *Chaplot et al.*, 2009; *Dlugoß et al.*, 2010]. As a result, in such areas there is commonly a strong correlation between topographic attributes such as slope angle or convexity with soil properties. Soil variability patterns are often mapped using digital soil mapping (DSM) methods [*McBratney et al.*, 2003]. After identifying and employing a statistical relation, DSM allows predicting soil properties or soil type using full-cover ancillary variables. Such ancillary variables are often derived from topographic and land cover attributes. DSM techniques have been applied successfully under a wide range of conditions [*Moore et al.*, 1993; *Gessler et al.*, 2000; *Tesfa et al.*, 2009].

[3] However, the fact that variability patterns can be mapped does not always mean that the causes of variability are known. In other cases soil properties cannot be predicted accurately because the relation between soil properties and ancillary variables is too weak. An example is the study by *Vanwalleghem et al.* [2010], who were not able to find accurate statistical relations to predict the starting depths of soil horizons from terrain attributes. In their case study in a natural forest area with loess-derived soils they mentioned local soil disturbances such as tree uprootings and variation in initial soil properties as possible causes that mask soil-landscape relations. In this paper we attempt to explain the poor terrain control on soil horizon depths in the same area by analyzing the effects of local disturbances in more detail and thus focus on loess-derived soils in a Belgian natural forest.

[4] Knowledge of the effect of tree uprooting on spatial soil variability is limited [*Šamonil et al.*, 2010, 2011], but effects on soil genesis (e.g., proxied by soil depth) have been demonstrated. In certain areas, the presence of pit-and-mound microtopography is a visible evidence of natural bioturbation processes. This microtopography is either caused by treefalls, for example in hummocky areas in the European

[1]Department of Geology and Soil Science, Ghent University, Ghent, Belgium.
[2]Departamento de Agronomía, Universidad de Córdoba, Córdoba, Spain.
[3]Department Earth and Environmental Sciences, KU Leuven, Leuven, Belgium.

Corresponding author: P. A. Finke, Department of Geology and Soil Science, Ghent University, Krijgslaan 281 S8, Ghent, East Flanders B-9000, Belgium. (peter.finke@ugent.be)

2169-9003/13/10.1002/jgrf.20153

Alps [*Embleton-Hamann*, 2004], or caused by burrowing animals like the mima mounds found in the northwestern U.S. [*Horwath and Johnson*, 2006]. *Schaetzl and Follmer* [1990] showed this pit-and-mound topography to be long lived and found evidence that dated some of these to over 2000 years. Whatever its origin, detailed soil transects have shown that this surface microtopography is reflected in the soil properties [*Embleton-Hamann*, 2004]. *Lutz and Griswold* [1939], *Armson and Fessenden* [1973], and *Beke and McKeague* [1984] mapped the soil profiles of pit-and-mound features and documented the disruption caused by treefalls, such as an A horizon sandwiched between two B horizons. *Langohr* [1993] described the importance of treefalls for interpreting soil stratigraphy in a geoarchaeological context. Also in areas without clear topographic evidence, bioturbation processes can control soil properties. *Phillips and Marion* [2004, 2005] and *Phillips* [2008] for example observed highly localized soil variability in a National Forest Area in the Ouachita Mountains, Arkansas. They concluded that biomechanical effects of trees on soil depth were highly significant. Trees may locally deepen the soil by exploring bedrock joints and fractures in bedrock soils. Treefalls then cause uprooting of bedrock material in shallow soils on bedrock or on unconsolidated sediments like loess or glacial till, resulting in homogenization of soil horizonation. *Gabet and Mudd* [2010], using a numerical soil redistribution model, showed that this uprooting process resulted in bedrock erosion rates that were consistent with observations in their study area in the Oregon Coast Range. In addition, they suggested that trees might have played a key role in the establishment of soil cover on rocky slopes. *Johnson et al*. [2005] focused on the effect of burrowing animals, describing how biota create a biomantle, characterized by a distinct zonation between an upper, biologically active and homogenized layer and an underlying layer. *Finke* [2012] showed in a model study that the hypothesis of *Phillips* [2007], wherein texture-contrasted soils may develop due to bioturbation, can indeed explain the texture contrast between E and Bt horizons. *Kaste et al*. [2007] indicated the relevance of bioturbation in contaminant transport, carbon sequestration, and landscape evolution at various time scales. Finally, *Gabet et al*. [2003] reviewed the importance of a wide range of bioturbation processes, from treefalls to the activity of burrowing animals, for sediment flux on hillslopes and soil production. For treefalls on slopes below 20°, they calculated sediment fluxes to be in the order of 10^{-4} to $10^{-3}\,m^3\,m^{-1}\,yr^{-1}$, which is typically an order of magnitude lower compared to sediment fluxes caused by soil erosion in agricultural landscapes. A recent study by *Hancock et al*. [2012] however concluded that the effect of treefalls on sediment fluxes is likely to be negligible as the pit-mound topography acts as sediment traps.

[5] While the above cited studies suggest that bioturbation is significant for soil fluxes and therefore for controlling overall soil depth, the effect of bioturbation processes such as treefalls on soil properties and on the spatial variability of individual soil horizons is largely unknown. Only for a few detailed case studies, the direct effect between bioturbation and soil horizonation has been investigated. A general process-based understanding is largely lacking although this piecewise evidence points to the importance of faunal and floral activities. A recent study by *Yoo et al*. [2011] explains how the vertical distribution of soil organic carbon in forest soils can be simulated well by a model that contemplates mixing by biota. *Finke* [2012] demonstrated in a modeling study the importance of bioturbation for the genesis of A, E, and Bt horizons. However, especially at the landscape scale, there is a knowledge gap about the effects of bioturbation on long-term soil formation processes and the resulting spatial soil variability. To a large extent, this can be attributed to the seemingly random nature of major bioturbation events like treefalls. We define "soil formation" as the change in soil properties over time that cause some primary (parent material) properties to disappear (e.g., sedimentary stratification in the topsoil) and secondary properties to develop (e.g., organic carbon content). These effects of soil formation are partly observable in the field as soil horizons.

[6] Initial variability in sediment properties may mask the effect of terrain controls on soil development. Here we focus on loess-mantled landscapes that widely occur in the temperate zone. Loess texture, mineralogy, and $CaCO_3$ content at sedimentation time are reported to vary, which may result in soil properties like decalcification depth (the depth to which the calcite has been dissolved due to acidic precipitation) not being related to current terrain properties. *Kowalinski et al*. [1972] and *Pye* [1983] identified weak spatial trends in loess texture in northwestern Europe and related this to distance to the source. Similar trends were observed in The Netherlands [*Mücher*, 1973], but differences are minor, which occur at spatial scales of 100 s of kilometers, and may be caused by local soil redistribution as well. At the scale of a forest catchment such as that studied by *Vanwalleghem et al*. [2010], we consider variation in fresh loess sediment composition of minor importance. Little is known on spatial trends in initial calcite content, but C horizon calcite contents in Weichsel loess have been reported between 2% [*Pye*, 1983] and more than 20% [*Wintle and Brunnacker*, 1982] at exposures across Europe. In summary, spatial variability in texture, mineralogy, and calcite content inside small areas is likely not related to the loess sedimentation but to post-depositional sediment and soil transport processes. Additionally, part of the loess may be of older age and already be decalcified at the time of deposition of the Weichsel loess. Both factors are not easy to reconstruct. Thus, exploration of the effect of variability in parent material as a cause of observed soil variability is, in most cases, only possible in a stochastic way.

[7] These uncertainties about the variability of initial sediment properties and bioturbation lead to the question to what extent soil-landscape relations, detected with DSM techniques, can be considered a resultant of (1) soil formation processes influenced by terrain position and (2) local random processes such as major bioturbation events and variability of the parent material properties.

[8] Application of a soil formation model at various locations in a landscape would inform about variability of soil properties caused by those local variations in soil-forming factors that are determined by relief. Inclusion in such a model of stochastic disturbances would inform about their additional effect on variability. We hypothesize that the SoilGen model [*Finke and Hutson*, 2008; *Finke*, 2012] allows the estimation of profile development as a function of local variations in soil-forming factors. This assumption is based on *Finke* [2012], who simulated a clear effect of topographic controls (slope and aspect) on decalcification depth and expression of Bt horizons, which was supported by soil analytical data. Additionally, this model can be run with stochastic

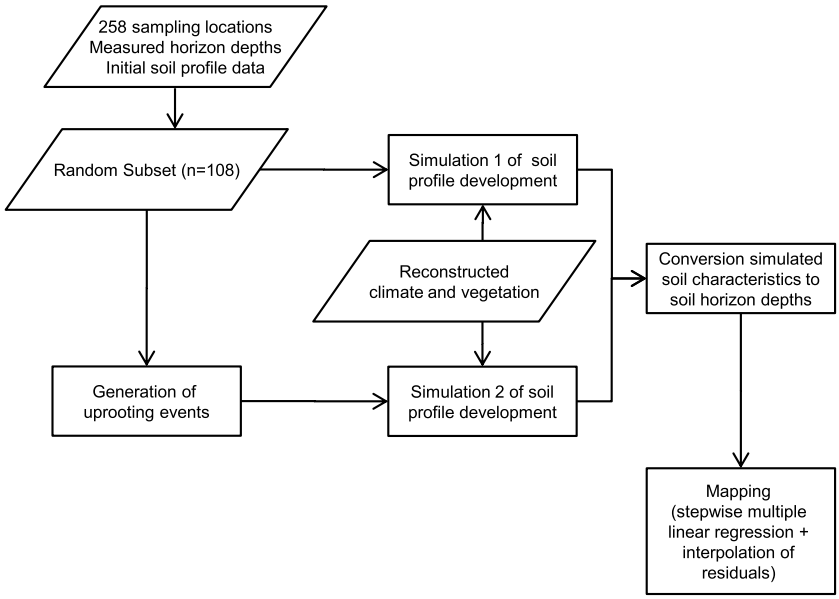

Figure 1. Flowchart of simulation and mapping activities (boxes) and used data (rhomboids).

inputs representing for instance the effect of treefalls. Therefore, we think the above question can, in principle, be answered in the setting of a simulation case study. We propose to apply this model in the context of the *Vanwalleghem et al*. [2010] study to identify the effects of treefalls on spatial variability of horizon depths, while comparing this variability to field observations. The simulation of the effect of variation of parent material properties is not considered for reasons of complexity and computational effort.

[9] The general objective of this work is therefore to analyze the effect of treefalls on soil formation and on the resulting spatial distribution of soil properties at the landscape scale and to compare results with observed soil variability. Specific objectives are as follows:

[10] 1. to apply the soil genesis model SoilGen to simulate soil development in loess-derived soils in a natural forest area in Central Belgium;

[11] 2. to convert simulated depth profiles of soil properties into soil horizon profiles;

[12] 3. to formulate and apply a partly deterministic, partly stochastic model to generate treefalls along the timeline and convert these to inputs of the SoilGen model; and

[13] 4. to analyze the relation between the current terrain, observed and simulated horizon thickness in case of the absence and presence of treefall events.

2. Materials and Methods

2.1. Study Area

[14] The study area is a natural, forested area in Central Belgium, called the Meerdaal forest (1329 ha). This area was selected because of the absence of human disturbance on the studied soil profiles. The forest is mentioned in early medieval documents which confirm that the area was forested at least since the mid-twelfth century. *Vanwalleghem et al*. [2003, 2005, 2006] showed evidence for a brief period of agricultural land use between the Middle Bronze Age and Roman times. This caused localized gully erosion but left the areas outside largely unaffected. The studied profiles are in these unaffected areas. After Roman times, the area was quickly reforested, as shown by sediment deposits [*Vanwalleghem et al*., 2006]. During Medieval times, the forest was mainly used for hunting. The forest is located in the Belgian loess belt. Local lithology is characterized by Quaternary loess deposits, mostly of Weichselian age [*Gullentops*, 1954] that overlie Tertiary marine sands of Middle to Late Eocene Age (52–36.6 Ma B.P.). The thickness of the loess layer is highly variable, ranging between 0 and 8.7 m, with an average thickness of 2.50 m [*Vanwalleghem et al*., 2010]. The original loess deposits are calcareous. Present-day loess samples reveal an average $CaCO_3$ content of 15% (±3%). The forest is managed as coppiced woodland whereby the larger trees are kept while the smaller undergrowth trees are harvested every 10–15 years. The current management consists of an increase in untouched forest reserve area (to 10% of the total area) and a gradual replacement of exotic species (several pine species) with native species managed in a low-impact silvicultural system. Forest regrowth is largely natural. Only tree species composition has been altered to some extent by silviculture during the last centuries. Current stands are dominated by oak species (*Q. robur L. and Q. petraea L.*) and beech on the loess-derived soils (*Fagus sylvatica L.*) (respectively, 57 and 18% of the area) with pine forest on the sandy outcrops (*Pinus sylvestris*, *Pinus nigra*, *and Pseudotsuga menziesii*). *Acer pseudoplatanus* is numerous in the understory of the stands where Quercus is dominating the overstory. Average stem number is 512 per ha [*De Keersmaeker et al*., 2009].

2.2. Research Layout

[15] This research focuses on 108 pedons in the Meerdaal forest. The locations were chosen randomly from a larger number of 258 where the depth to Eocene sands was measured by soil augerings in an earlier study [*Vanwalleghem et al*., 2010] and an overlying loess cover was present. Horizon thicknesses have been estimated by these authors in the field. The 108 pedons are a compromise between a sufficient number to perform spatial analyses [*Webster and*

Oliver, 1992] and a feasible simulation effort. Two scenarios are simulated for each location (Figure 1): (i) natural soil development, starting at 15,000 B.P. with a parent material consisting of the C horizon of the loess on top of Eocene marine sand and ending at 0 B.P. and (ii) natural soil development including occurrences of soil disturbance due to uprooting of trees. With "natural soil development" we mean that direct human influences such as those related to agricultural land use are excluded and a natural vegetation development is assumed. As stated above and in more detail by *Vanwalleghem et al*. [2010], this is likely the case in the Meerdaal forest with the exception of localized and short-spelled agricultural activities between the Middle Bronze Age and the Roman era. These activities have led to the formation of some gullies in the area, but the 108 pedons are all outside these areas.

[16] In order to compare model results with field observations, simulated soil characteristics like organic carbon (OC) and clay content at 0 B.P. are converted to horizon thickness according to a protocol developed during this study and based on both measured and simulated soil data. Regression kriging is then used to characterize the soil-landscape relationship in an approach similar to *Vanwalleghem et al*. [2010]. Resulting horizon thicknesses from the two simulated scenarios are first correlated to terrain variables using stepwise multiple linear regression techniques to evaluate the effect of tree uprootings on the predictive quality by this digital soil-mapping technique. Next, ordinary kriging is used to interpolate the residuals of the regression model, and a map would be produced by adding the regression predictions and interpolated residuals. In this case, we are only interested in exploring the spatial correlation in the data by analyzing the semivariograms of the residuals.

[17] The spatial differences between the 108 pedons at 0 B.P. in simulation scenario 1 (hereafter referred to as model 1) can be considered the deterministic response of soil formation processes to initial variation in thickness of loess cover and site aspect only, as all other factors (initial conditions and inputs along the timeline) are kept constant. As such, we expect a strong statistical relation between simulated horizon thicknesses and terrain attributes. The spatial differences in simulation scenario 2 (hereafter referred to as model 2) should be partly attributable to the effect of tree uprootings over time, which is considered a probabilistic process because there is no mechanistic method to predict uprootings. Therefore, we expect a weakened statistical relation between simulated horizon thicknesses and terrain attributes. The research layout aims at identifying how much the relation weakens because of treefalls and how this compares to the relations based on measured soil horizon thickness.

2.3. SoilGen Model

[18] The current study was done using SoilGen2.16, documented in *Finke* [2012] and downloadable from http://users.ugent.be/~pfinke/index_bestanden/SG216.zip. SoilGen is a soil genesis model that describes various soil physical and soil chemical processes. It is a 1-D vertical transport model in the sense that it simulates unsaturated water flow by the Richards' equation, solute transport by the convection-dispersion equation and soil temperature by the heat flow equation. Main properties of this approach are described in detail by *Finke and Hutson* [2008], and this part of the model is based on the Leaching Estimation and Chemistry Model [*Hutson*, 2003]. Additionally, SoilGen models the CO_2 diffusion in the gas phase and the physical disintegration of soil particles caused by temperature fluctuations. Mass transport between soil compartments can also occur as a result of bioturbation and by clay migration [*Finke*, 2012]. These changes are used to annually update soil hydraulic characteristics by pedotransfer functions. The chemical system of SoilGen includes Ca, Mg, Na, K, Al, and H in the exchange phase; $Al(OH)_3$, $CaCO_3$, and $CaSO_4$ in the precipitated phase; Ca^{2+}, Mg^{2+}, Na^+, K^+, Al^{3+}, H^+, OH^-, Cl^-, SO_4^{2-}, HCO_3^-, and CO_3^{2-} in the solution phase and as part of four organic C pools (decomposable plant material, resistant plant material, biomass, and humus). The C cycle is modeled similarly to RothC-26.3 [*Coleman and Jenkinson*, 2005] but for every soil compartment separately and for several vegetation types. One addition is that uptake of ions by the plants follow the same decomposition pathways as C, to be ultimately released again in the solution phase. Chemical equilibrium constants between various species in solution and precipitated phases are modified by the Arrhenius temperature correction of standard values at 25°C using documented activation energy and simulated soil temperature. Furthermore Ca, Mg, Na, K, and Al occur in the unweathered mineral phase from which they are slowly released by chemical weathering. The system and transfers between pools are described in detail by *Finke and Hutson* [2008] and *Finke* [2012].

[19] SoilGen2.16 identifies four vegetation types (grass/scrubland, coniferous wood, deciduous wood, and cereal-type agriculture); each of them are having a characteristic root distribution pattern, water uptake, and ion uptake according to a forcing function and C mineralization with associated ion release [*Finke*, 2012].

[20] Bioturbation is modeled as an incomplete-mixing process. Each soil compartment (for instance of 5 cm thickness) that is subject to bioturbation contributes a depth-dependent input mass fraction to a bioturbation pool, which is then mixed (vertical mixing). Next, the bioturbation pool is redistributed over the soil compartments according to the input mass fractions, and horizontal mixing is done with the remaining mass per compartment. This method is applied to all soil components that can be expressed as mass, including solutes, soil water, exchanged cations, precipitated salts, weatherable minerals, and carbon pools. This approach mimics the behavior of geophagous macrofauna, like earthworms. Bioturbation values are scarce and are usually taken from literature. The effect of plowing, or of a treefall, is simulated as an intensive form of bioturbation.

[21] Various subprocesses in SoilGen have been calibrated and were compared to measurements. Calibration of the calcite dissolution coefficient was done by *Finke and Hutson* [2008] and *Finke* [2012] on Belgian loess soils. Physical weathering and clay migration were calibrated by *Finke* [2012]. Recently [*Yu et al*., 2012], the C cycle submodel was calibrated for deciduous forests in Belgium and China. Model quality testing was done for loess-derived soils in Belgium and China and for a marine clay chronosequence in Norway [*Sauer et al*., 2012].

[22] The effect of aspect and slope angle on soil development is one of the few spatially varying factors in the current study (beside the effect of a varying thickness of the loess cover). This topographic effect is used in SoilGen to adjust the annual precipitation and evapotranspiration.

Table 1. Inputs for the SoilGen Model and Associated Data Sources

Group	Input Variable or Parameter	Dimensions	As Initial Condition	Time Series, in Typical Year	Time Series, Annual	Source for Data and/or Method
Climate	Temperature	°C	Yes	Weekly average and daily amplitude	January and July averages	*Davis et al*. [2003], *Finke and Hutson* [2008], *Godefroid and Koedam* [2010]
	Precipitation	millimeter	-	Daily depth, intensity, and chemical composition of rain	Annual sum	*Davis et al*. [2003], *Finke and Hutson* [2008]; Uccle weather data
	Potential evapotranspiration	millimeter	-	Weekly total	Annual sum	*Hargreaves and Samani* [1985], *Finke and Hutson* [2008]
Organisms	Vegetation type	-	-	-	Vegetation type, rooting depth, and C input as litter	*Verbruggen et al*. [1996]
	Bioturbation	$kg.1000\,ha^{-1}\,y^{-1}$	-	-	Yearly depth distribution	*Finke* [2012]
Relief	Slope angle	degree	Yes			DEM; *Vanwalleghem et al*. [2010]
	Slope aspect	degree	Yes			DEM; *Vanwalleghem et al*. [2010]
	Wind direction	degree	Yes			*Godefroid and Koedam* [2010]
Parent material (for loess and Eocene sand)	Clay/Silt/Sand	Mass %	Yes			Loess: 6.4/81.6/12.0% Eocene: 1.4/0.6/98.0% *Vanwalleghem et al*. [2010]
	OC	Mass %	Yes			0.1% assumed
	Ca, Mg, Na, K, Al, SO_4, Cl, Alkalinity in solution	$mmol\,dm^{-3}$	Yes			Unpublished data from analyzed C horizon in Meerdaal forest
	Ca, Mg, Na, K, Al, H on exchange complex and CEC	$mmol^{+}\,kg^{-1}$	Yes			Unpublished data from analyzed C horizon in Meerdaal forest
	$CaCO_3/CaSO_4$	Mass %	Yes			15/0% *Vanwalleghem et al*. [2010]
	Gapon exchange coefficients	$(mol\,dm^{-3})^{1/}_{n-1/m\ a}$	Yes			*De Vries and Posch* [2003]
	Ca, Mg, Na, K, Al in primary minerals	$mol^{+}\,kg^{-1}$	Yes			V. Ranst (Ghent University, unpublished PhD thesis, 1981)

[a] n and m are the charges of the ion pair involved.

[23] The size and bearing of a slope in combination with the speed and direction of the wind carrying the precipitation affect the net precipitation received by a unit area [*Lyles et al*., 1969]. To calculate the net effect of wind speed, slope angle, and their bearings on precipitation, first the wind speed in the direction of the slope is calculated:

$$V_2 = V_1 \cos(\delta - \gamma), \tag{1}$$

where V_2 ($m\,s^{-1}$) is the wind speed in slope direction, V_1 ($m\,s^{-1}$) is the wind speed in the wind direction, δ is the upslope bearing (°, equivalent to aspect + 180°), and γ (°) is the downwind direction.

[24] The diversion angle β (°) from vertical rainfall induced by wind is calculated according to *Mauersberger* [2001, p.30]:

$$\beta = \mathrm{abs}\left(\arctan\left({}^{V_2}/_{V_r}\right)\right), \tag{2}$$

where V_r ($m\,s^{-1}$) is the mean fall velocity of raindrops (e.g., estimated from rainfall intensity) [*Schmidt*, 1992, p.412]. In SoilGen, V_r has the fixed value of $5\,m\,s^{-1}$.

[25] The rainfall depth R_2 (mm) on a sloping area of $1\,m^2$ with slope angle α, wind effect β, and their bearings δ and γ, respectively, is then given by [*Erpul et al*., 2008]

$$R_2 = R_1(1 + \tan(\beta)\tan(\alpha)\cos(\delta - \gamma)), \tag{3}$$

where R_1 (mm) is the precipitation depth at the horizontal plane.

[26] The potential evapotranspiration PE_2 is a correction of the measured PE_1 for latitude, slope angle, and slope azimuth, assuming that potential evapotranspiration responds linearly to differences in incoming radiation for different slopes. Then, the correction factor is the ratio between the potential solar radiation on a horizontal surface at given latitude, summarized for 1 year, and the potential solar radiation on a slope α with upslope bearing δ converted to map area for the same period. This ratio was calculated with an implementation of an algorithm developed by *Swift* [1976].

2.4. Model Inputs

[27] Each input parameter for SoilGen can either be a process parameter, an initial value, or a boundary condition varying in time. We took the process parameters that were calibrated and estimated by *Finke* [2012] as this preceding

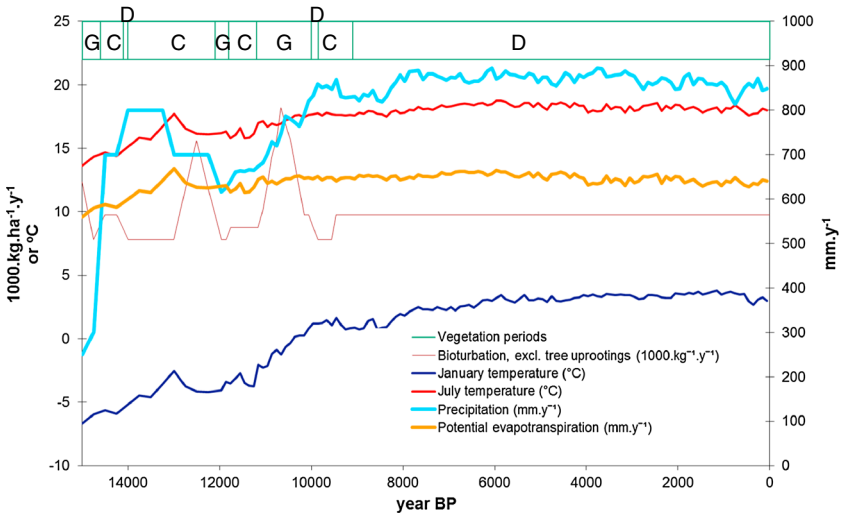

Figure 2. Boundary conditions for the soil modeling, representing reconstructed climate and vegetation change over the last 15,000 years. G = Grassland, C = Coniferous forest, D = Deciduous forest. For data sources, see Table 1.

study was done on loess-derived soils nearby the Meerdaal forest. Table 1 summarizes the parameters and some of their initial values and identifies if time series were reconstructed for boundary inputs along the timeline. Figure 2 visualizes these boundary inputs. The boundary inputs were assumed spatially constant for all simulated plots, although via the relief and aspect, the inputs precipitation and potential evapotranspiration are corrected at the plot level according to the method described in the previous section.

2.5. Transforming Simulated Soil Parameters to Horizon Thickness

[28] During the field inventory by soil augering [*Vanwalleghem et al.*, 2010], the depths of transition between occurring major soil horizons were recorded: A (mineral, humus-rich horizon), E (eluvial horizon, in this case study indicating loss of clay), Bt (illuviation horizon with increased clay content), BC (transitional horizon with limited clay illuviation), C1 (decalcified loess), and C2 (calcareous loess). Also, the depth to the underlying Eocene marine sand (C3) was noted, and all augerings reached to this depth. A typical horizon sequence is thus A-E-Bt-BC-C1-C2-C3. Horizon codes were assigned in the field based on soil color, expert estimations [*Food and Agriculture Organization* (*FAO*), 2006] of organic matter content and clay content, and presence of $CaCO_3$ as shown by effervescence with hydrochloric acid. All profiles were described by the same person. As the SoilGen model calculates soil properties like clay content, carbon content, and $CaCO_3$ content at all soil compartments *i*, these values at simulation time 0 B.P. have to be translated to current horizon codes. Vertical compartment size in SoilGen was set to 5 cm. Horizon codes can be obtained by transforming

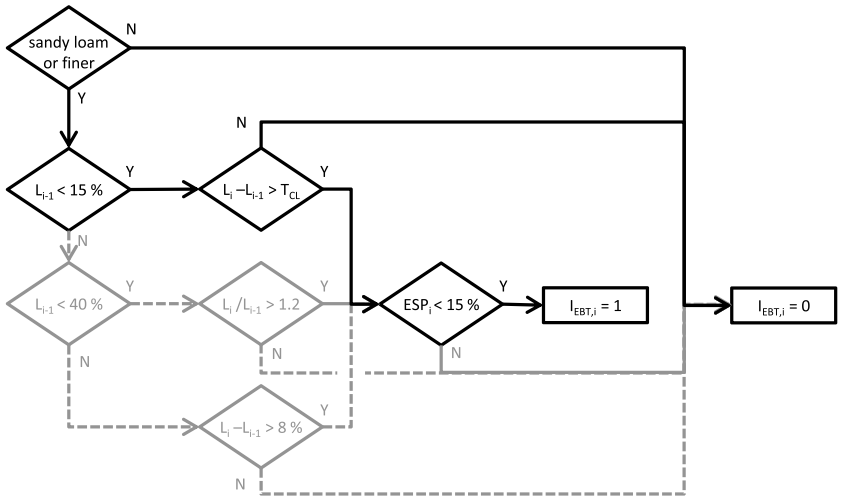

Figure 3. Decision tree to decide if a E/Bt horizon transition is present in compartment *i*, using an indicator value $I_{BT,i}$ based on *L* (Lutum, clay content, %), ESP (Exchangeable Sodium Percentage), and a threshold value for depth change in clay content (T_{CI}). Solid black lines indicate (simulated) situations occurring in the study area; dashed grey lines indicate non-occurring situations.

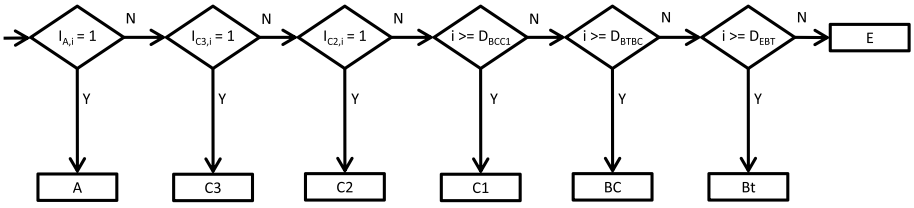

Figure 4. Decision tree to decide what horizon occurs at the depth of compartment *i*. *I* and *D* describe the presence of a horizon and transition depth to another horizon, respectively. For the derivation of *I* and *D*, see text. A, C2, C1, BC, and Bt are horizon codes [*FAO*, 2006], and C3 indicates the Eocene marine sand below the loess.

relevant simulated soil properties to indicators for horizons (or horizon transitions) by comparison to threshold values for these properties. Threshold values for each indicator can iteratively be estimated by minimizing the average difference in horizon depths based on indicator values and the measured depths over all soil profiles that contain the horizon in the field. By calibrating the threshold values (indicated with *T*), we compensate for unknown bias in the field estimates to identify soil horizons and also for the fact that the SoilGen model was not calibrated for the Meerdaal forest. We propose the following decision rules to obtain indicator values for horizon codes (default values for indicators (*I*) are 0, for transition depths (*D*) −999; ∀ means "for all"):

[29] 1. $\forall\ OC_i \geq T_{OC} : I_{A,i} = 1$, where OC is simulated organic carbon (%) and T_{OC} is a threshold value for OC. This defines all compartments belonging to the A horizon;

[30] 2. $\forall (L_i - L_{i-1}) \geq T_{CI} : I_{EBT,i} = 1$ (see decision tree in Figure 3), where L is simulated clay (Lutum) percentage and T_{CI} is a threshold Clay percentage increase; analogous to application of the world reference base criteria 1, 2, and 4 [*International Union of Soil Science Working Group WRB*, 2006, p.13–14] for the *argic* diagnostic horizon. $I_{EBT,i}$ defines the transition depth D_{EBT} between the top of the Bt horizon and the bottom of the E horizon. All compartments between the A horizon and the top of the Bt horizon are considered part of the E horizon;

[31] 3. $\forall ACDI_i < T_{CDI} : I_{BtBC,i} = 1$, where $ACDI_i$ is the Average Clay Dispersion Indicator for compartment *i* over all simulated years. The Clay Dispersion Indicator (CDI) in a compartment at a particular simulation year has the value 0 if there is calcite or gypsum present or if the electrolyte concentration (EC) ≥ critical salt concentration (CSC) as defined in *Finke* [2012]. In all other cases, the CDI has the value $(1 - EC/CSC)$. T_{CDI} is a threshold value for CDI. ACDI indicates the likelihood that clay migration has occurred in a particular compartment over total simulation time. The lower the value of ACDI, the longer the period that flocculating conditions prevailed or the shorter the period of clay dispersion conditions (inhibiting the movement of clay into or out of that compartment). $I_{BtBC,i}$ defines the transition depth (D_{BtBC}) of the Bt and the BC horizons.

[32] 4. $\forall (L_{i,t=T} - L_{i,t=0}) > T_{Ctol} : I_{BCC1,i} = 1$, where the increase in clay content (L) between 15,000 B.P. ($t = 0$) and present ($t = T$) is compared to a tolerance threshold clay content T_{Ctol}. $I_{BCC1,i}$ defines the transition depth (D_{BCC1}) between the BC horizon and the top of the horizon below, usually the decalcified C1 horizon.

[33] 5. $\forall (\ Calcite_{i,t=0} - Calcite_{i,t=T}) < T_{calctol} : I_{C2,i} = 1$, where the initial calcite content at $t = 0$ is based on measurements (Table 1). $I_{C2,i}$ identifies all compartments belonging to the (calcareous) C2 horizon. As the decalcification front is very sharp, $T_{calctol}$ can be expected to be close to the initial calcite content. However, because SoilGen is not calibrated to the sites in the Meerdaal forest, there may be systematic differences between simulated and measured depths to the C2 horizon as the annual percolation is uncertain. This is caused by an unknown fraction of the rain that is lost by forest interception [*Finke*, 2012].

[34] 6. $\forall (i > C3_x)$: $I_{T,i} = 1$. The depth C3 of the Eocene marine sand underlying the loess is known for each location *x*.

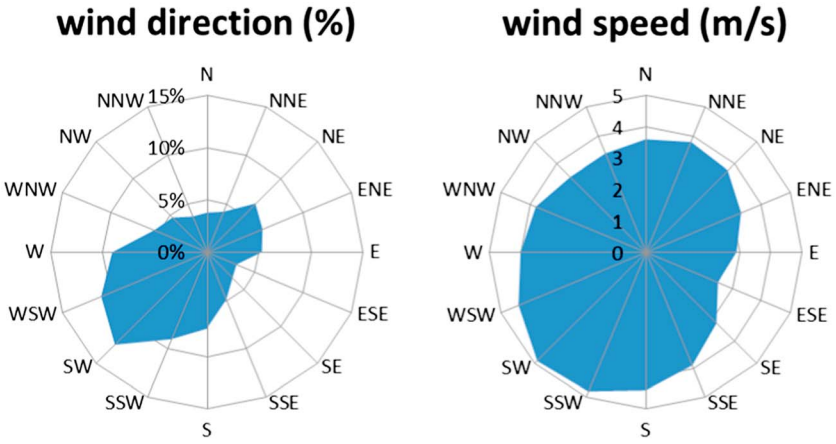

Figure 5. Annual distributions of wind direction and wind speed for Uccle, Belgium, used to feed the stochastic tree-uprooting model.

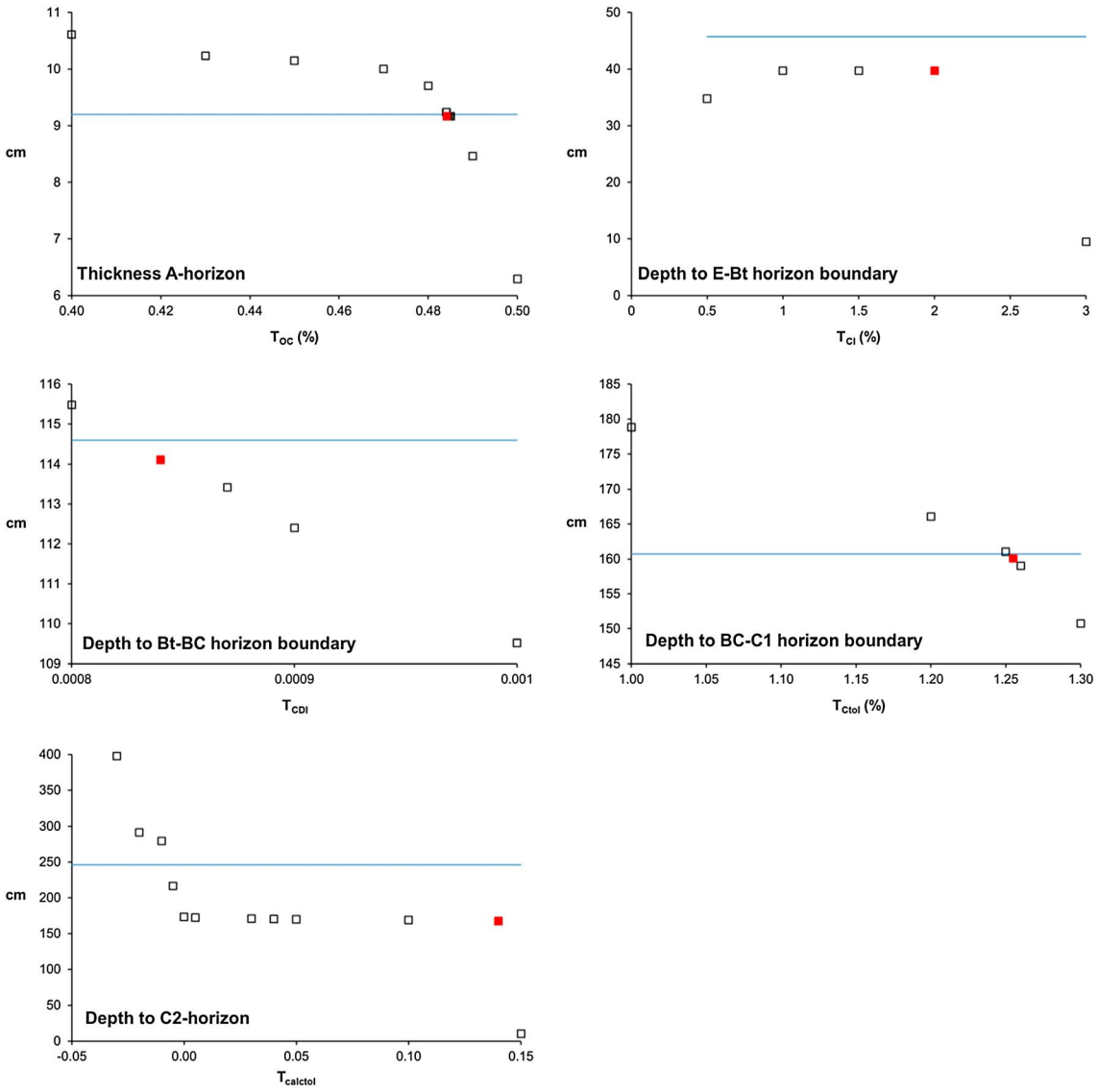

Figure 6. Calibration of threshold values (T) of simulated soil properties to match estimated and measured thickness or depth to five soil horizons. Solid blue lines indicate average measured values, open symbols indicate average estimated values at various thresholds. Filled red symbols indicate chosen values for T. Note that negative values for T_{calctol} indicate calcite accumulations.

[35] After the threshold values T have been obtained by calibration, assignment of horizon codes to soil compartments is straightforward (Figure 4).

2.6. Generating Uprooting Events

[36] Tree uprooting has long been identified as a factor disturbing the topsoil layers and thus affecting soil genesis [*Schaetzl et al*., 1989; *Ulanova*, 2000; *Phillips*, 2008]. Various factors have been named as causes for tree uprooting: strong winds, wind exposure, soil wetness, and the general condition of the tree as determined by possible disease and age. Empirical studies have identified disturbance cycles (expected number of years between successive treefall events at a location in a forest stand) [*Schaetzl et al*., 1989] and relation to wind exposure [*Maxwell et al*., 2010] in case studies. This does not mean that tree uprooting can be predicted with high confidence for individual trees, and thus the likelihood of tree uprooting at the scale of a pedon in a certain year can at best be estimated. We therefore propose a probabilistic approach to predict the occurrence of tree uprooting in a certain year at pedon scale. This probabilistic approach is based on empirical studies worldwide in similar natural forests as were present in the studied loess area in Belgium. Basically, the probability of a treefall is derived from the disturbance cycle (the average time between two tree uprootings in a soil pedon). The disturbance cycle is modified by a factor describing the effect of wind exposure to obtain a site-specific probability which is subsequently corrected to obtain the probability of treefalls (P_{treefall}) that result in uprooting:

[37] 1. From *Schaetzl et al*. [1989] we take the disturbance cycle from Illinois of 1730 years, so $P_{\text{treefall}} = 1/1730$;

[38] 2. We calculate the modified treefall probability $P_{\text{treefall},x}$ by multiplying P_{treefall} with a wind exposure factor WE_x at position x;

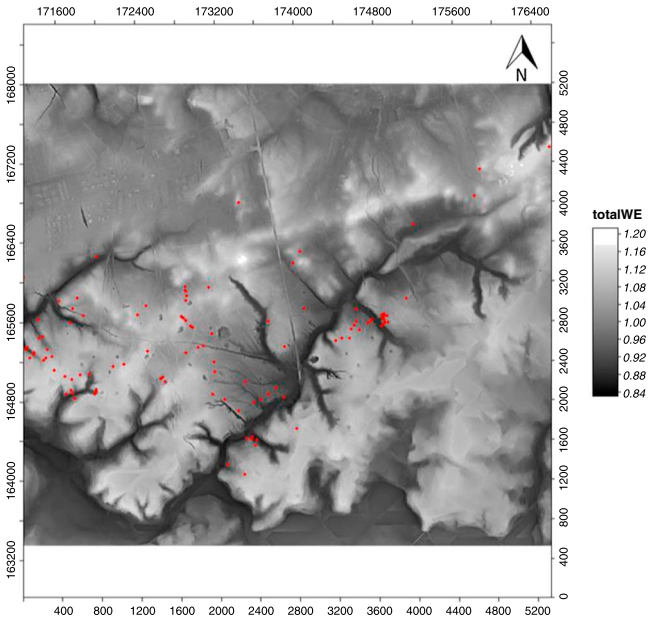

Figure 7. Average annual wind exposure (totalWE) for Meerdaal forest and its surroundings calculated with distributions of wind direction, wind speed, and the DEM. TotalWE values exceeding 1 indicate luff effects (windward slope exposure); those values less than 1 indicate a lee effect. Red dots indicate 108 simulation locations with measured horizon thickness. Axis numbers indicate Lambert 2 coordinates (m).

A map of the wind exposure factor is obtained by calculating the wind exposure for the digital elevation model (DEM) of the Meerdaalwoud for all wind directions (at 16 intervals of 22.5°) and associated wind speeds as documented for the nearby Uccle weather station (Figure 5). The SAGA 2.0.8 "wind effect" module is used. An average wind exposure map is then obtained by weighting the resulting 16 maps for the frequency of occurrence of the wind speed.

[39] 3. Following *Maxwell et al.* [2010], we assume that 85% of treefalls cause uprooting (15% are broken stems and assumedly do not disturb the soil);

[40] 4. In any year y in which a forest vegetation is present, we decide if a treefall event with uprooting $WU_{y,x}$ occurs at a location x by generating a random number R_y [0;1] and applying the rule ($\wedge$ means "as well as"):

$$WU_{y,x} \;\forall\; R_y < 0.85\; P_{\text{treefall},x} \;\wedge\; (\text{no treefall last 70 years}) \;\wedge\; (\text{forest older than 70 years})$$

The last two conditions were added because uprootings of young trees (arbitrarily set to younger than 70 years) are assumed not to affect the soil.

[41] 5. Following *Ulanova* [2000], we take that the bioturbation in the year of a treefall affects the upper 80 cm. We interpret this as instantaneous near-complete mixing: 95% of the soil mass corresponding to this depth interval is mixed in the year of an uprooting event. As such, we do not take into account that a pit-mound topography may temporarily exist at the location of a treefall, which is gradually leveled but instead assume immediate leveling, which is a simplification of reality.

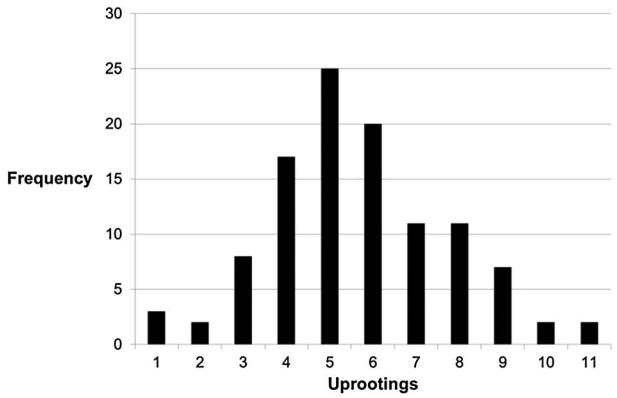

Figure 8. Frequency distribution of simulated tree uprootings at 108 locations within Meerdaal forest during the simulation period (15,000–0 years B.P.).

2.7. Geostatistical Analysis

[42] The geostatistical analysis done by *Vanwalleghem et al.* [2010] was repeated for the reduced observation data set of 108 points (pedons) and for both simulated data sets (models 1 and 2) at the same locations. Regression kriging was used to produce a spatial prediction model for the thickness of each soil horizon. Regression kriging is a hybrid approach that combines a multiple linear regression model with ordinary kriging [*Odeh et al.*, 1994]. First, a (multiple) regression model between observed values and (multiple) full-cover environmental variables is fitted. Second, the residuals between the regression predictions and observed values are mapped by ordinary kriging. The full-cover regression predictions and mapped residuals are then added to obtain a full-cover map. If no spatial structure is present in the residuals, the model reduces to a simple regression

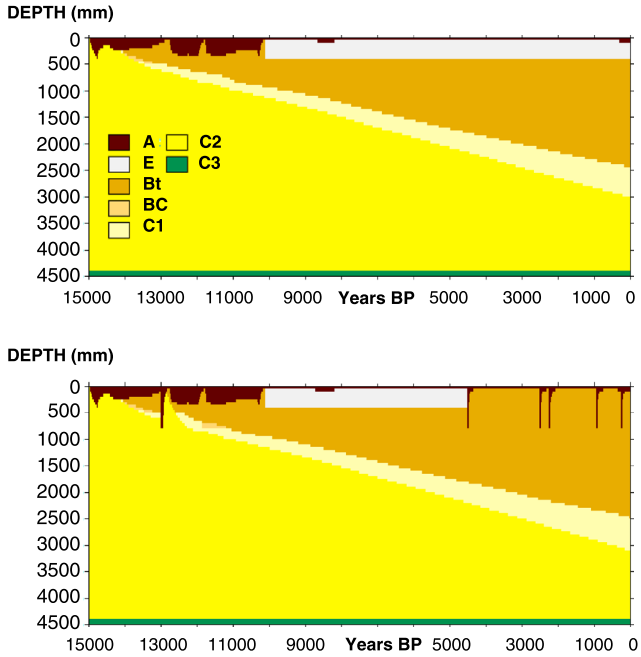

Figure 9. Example result of simulated soil horizon (A, E, Bt, BC, C1, C2, and C3) development on loess over time (15,000–0 years B.P.) using (top) model 1 (no treefalls) and (bottom) model 2 (6 treefalls). Note that profile thickness is 4.50 m.

Table 2. Summary Statistics for the Relations Between Spatial Covariates and Observed Data, Model 1 and Model 2

		Observed Data					Model 1 No Tree Uprooting					Model 2 Including Tree Uprooting				
		Soil Horizon					Soil Horizon					Soil Horizon				
	Covariate	E	BT	BC	C1	C2	E	BT	BC	C1	C2	E	BT	BC	C1	C2
Regression Model	*n*	70	84	77	77	68	95	105	68	39	108	0	104	47	59	107
							I. Univariate Model[a]									
Landscape attributes	Slope angle	-	-	-	-	-	-	-	0.15 (0.001)	0.24 (0.002)	-	NP	-	-	0.1 (0.02)	-
	Profile curvature	-	-	-	-	-	-	-	-	-	-	NP	-	-	-	-
	Plan curvature	-	-	-	-	-	-	-	-	-	-	NP	-	-	-	-
	Log(Wetness Index)	0.07 (0.02)	-	-	0.08 (0.01)	-	-	-	-	0.21 (0.003)	-	NP	-	-	-	-
	Loess thickness	0.08 (0.02)	-	-	0.06 (0.03)	-	0.18 (<0.001)	0.28 (<0.001)	-	0.16 (0.01)	0.04 (0.03)	NP	-	-	-	0.05 (0.02)
	Soil	-	-	-	0.22 (0.007)	-	0.21 (0.002)	0.45 (<0.001)	-	-	0.15 (0.01)	NP	-	0.23 (0.02)	0.24 (0.02)	0.14 (0.02)
	Landform	-	-	-	-	-	-	-	-	-	-	NP	-	-	-	-
	Aspect	-	-	-	-	-	0.1 (0.019)	-	0.58 (<0.001)	0.3 (0.005)	0.39 (<0.001)	NP	-	0.47 (<0.0001)	0.64 (<0.0001)	0.35 (<0.0001)
							II. Multiple Regression Model[b]									
Intercept		0.15	0.48	1.22	1.69	2.42	0.08	0.24	−297.5	326.9	2.06	NP	-	1.03	1.03	2.14
Landscape attributes[c]	Slope	-	-	-	-	-	-	-	−0.01	0.02	-	NP	-	-	0.02	-
	Profile curvature	−0.0004	-	-	-	-	-	-	-	-	-	NP	-	-	-	-
	Plan curvature	-	-	-	-	-	-	-	-	-	-	NP	-	0.005	-	-
	Log(Wetness Index)	-	-	-	-	-	-	-	21.5	−27.1	-	NP	-	-	-	-
	Loess thickness	-	-	-	-	-	0.004	0.016	-	-	−0.05	NP	-	-	-	−0.06
Land form	Landf (2&1−3)	-	−0.04	-	-	-	-	-	-	-	−0.12	NP	-	-	-	-
	Landf (2−3&1)	-	-	-	-	-	−0.004	-	-	-	-	NP	-	-	-	-
	Landf (1−2&3)	-	-	-	-	-	-	-	−0.08	-	-	NP	-	-	-	−0.12
Soil	Soil (1&3−2)	-	-	-	-	-	-	-	-	-	−0.44	NP	-	-	-	−0.46
	Soil (1−5&6)	-	-	-	-	-	-	-	−0.16	-	-	NP	-	-	-	-
	Soil (4&3&2−1&6&7&5)	-	-	-	−0.17	-	-	-	-	-	-	NP	-	-	-	-
	Soil (7&4&3&2−1&6)	-	-	−0.11	-	-	-	-	-	-	-	NP	-	-	-	-
	Soil (3−1&2&4&5&6&7)	-	-	-	-	-	−0.007	-	-	-	-	NP	-	-	-	-
	Soil (1−2&3&4&5&6&7)	-	-	-	-	-	-	−0.09	−0.09	-	-	NP	-	-	-	-
	Soil (4&5&6&7−1&2&3)	-	-	-	-	-	-	-	-	-	−0.33	NP	-	-	-	−0.32
	Soil (1&3−2&4&5&6&7)	-	-	-	-	−0.12	-	-	-	-	-	NP	-	-	-	-
	Soil (1&6&7&3&4−2)	−0.05	-	-	-	-	-	-	-	-	-	NP	-	-	-	-
	Soil (1&6&7−4&3)	-	-	-	-	-	-	-	-	-	-	NP	-	−0.13	-	-
	Soil (1&5&6−7&3&4)	-	-	-	-	-	-	-	−0.14	-	-	NP	-	-	-	-
	Soil (1&5&6−7&4&3&2)	-	-	-	-	-	-	-	-	-	-	NP	-	-	−0.15	-
Aspect	Aspect(1)	-	-	-	-	-	-	-	0.045	-	-	NP	-	-	-	-

Table 2. (continued)

Regression Model	Observed Data						Model 1 No Tree Uprooting						Model 2 Including Tree Uprooting					
	Soil Horizon						Soil Horizon						Soil Horizon					
Covariate	E	BT	BC	C1	C2		E	BT	BC	C1	C2		E	BT	BC	C1	C2	
n	70	84	77	77	68		95	105	68	39	108		0	104	47	59	107	
Aspect(2)	-	-	-	-	-		-	-	−0.36	-	-		NP	-	-	-	-	
Aspect(3)	-	-	-	-	-		-	-	−0.031	-	-		NP	-	-	-	-	
Aspect (2–3)	-	-	-	-	-		-	-	−0.17	-	−0.16		NP	-	−0.16	-	−0.13	
Aspect (1–4)	-	-	-	-	-		-	-	−0.17	-	-		NP	-	−0.11	-	-	
Aspect (1&3&4–2)	−0.01	-	-	-	-		-	-	-	-	-		NP	-	-	-	-	
Aspect (4&1–2&3)	-	-	-	-	-		−0.005	−0.01	-	-	-		NP	-	-	-	-	
Aspect (2&3–4&1)	-	-	-	-	-		-	-	−0.19	−0.31	−0.31		NP	-	-	−0.48	−0.3	
$r^2_{adjusted}$	0.18	0.04	0.07	0.19	0.06		0.38	0.53	0.73	0.60	0.49		NP	-	0.59	0.71	0.44	
Prob > *F*	0.0036	0.04	0.01	<0.0001	0.05		<0.0001	<0.0001	<0.0001	<0.0001	<0.0001		NP	-	<0.0001	<0.0001	<0.0001	

[a] Only significant relations are indicated. The first value is the fraction of the variance explained by the predictor variable. Values between brackets are critical p values (p^*). p^* is Prob > t for the linear regression on the continuous variables. p^* for the categorical variables is Prob > F in the one-way analysis of variance test.

[b] For the multiple regression models, the regression equation coefficients and the total model performance is indicated.

[c] Categorical variables result from the hierarchical approach applied in JMP, Version 7, SAS Institute Inc. and should be interpreted as follows: e.g., Landf(2–3&1&4) combines the levels that are most alike to obtain two groups that are most different (2 versus 1, 3, and 4). In case of landform class = 2, this variable obtains the value + 1, otherwise − 1.

[d] Prob > F = significance level associated with the F statistics.

NP = Not Present (according to protocol).

model. If no (multiple) linear statistical relation is present between soil horizon depth and environmental variables, the model reduces to ordinary kriging. Spatial correlation in the observed and simulated soil profiles was assessed by analysis of the semivariogram, which was constructed by using either the residuals, in case a regression model could be established, or else the soil horizon depth data directly. Most of the full-cover environmental variables are derived from a DEM. The "wetness index" is equal to the compound topographic index defined by *Beven and Kirkby* [1979]. Statistical analysis was performed with JMP version 7, SAS Institute Inc., Cary, NC, 1989–2007. Semivariogram analysis was done with Vesper version 1.6. [*Whelan et al*., 2001].

3. Results

3.1. Simulated Horizon Thickness

[43] The results of the calibration of the threshold values to derive depths and thickness of horizons from the model outputs are given in Figure 6. The average field thickness of the A horizon (108 field locations), depth to the boundary between Bt-BC (77 field locations) and BC-C1 (78 field locations) could be well reproduced by selecting an adequate threshold value. The depth of the E-Bt transition (84 field locations) was best approached by a clay content contrast between E and Bt (T_{Cl}) of 2%, which gives a small (5 cm) bias between average measured and simulated depths that could be bridged by calibration of the model (likely via the depth of bioturbation) but that could equally well be the result of bias because of the augering technique used in the field. The depth to the decalcification front (C1-C2 transition, 68 locations) was coupled to a $T_{calctol}$ of 0.14 (maximum 1% of the 15% calcite remaining). The figure shows that for negative values of $T_{calctol}$, the average measured value can be reproduced, but negative values indicate calcite accumulation zones in the C2 horizon, which occurred only in one simulation. Choosing $T_{calctol}$ of 0.14 implies a bias of 78.4 cm underestimation of the depth of C1-C2 transition by simulations, which might be bridged by calibration of the model (likely via the fraction of rain intercepted by forest). However, bias in the estimation of absolute horizon depths is not of great importance as it becomes part of the regression constant in the stepwise multiple linear regression with terrain attributes. More important is the spatial structure and the relation with terrain attributes of the simulated soil horizon depths, which is not affected by this bias.

3.2. Uprooting Events

[44] Figure 7 shows the total wind exposure over a typical year for the DEM of the Meerdaal forest. Besides the wind exposure of the natural relief, also that of roads and built-up structures is visible, especially to the north. However, the simulation locations are always outside the distance of influence of these nonnatural relief features. The wind exposure factor over all 108 sites varies between 0.87 and 1.13 for leeward sites and windward sites, respectively, with an average of 1.01. The protocol to calculate tree-uprooting events produced a total of 614 uprootings, varying between 1 and 11 uprootings per site (Figure 8) over 12,461 years of forest vegetation. This number depended on probability and wind exposure and was equivalent to an average disturbance cycle of $108 \times 12641 \times 0.85/614 = 1890$ years (0.85 is the fraction of treefalls causing uprooting; see section 2.6). This number

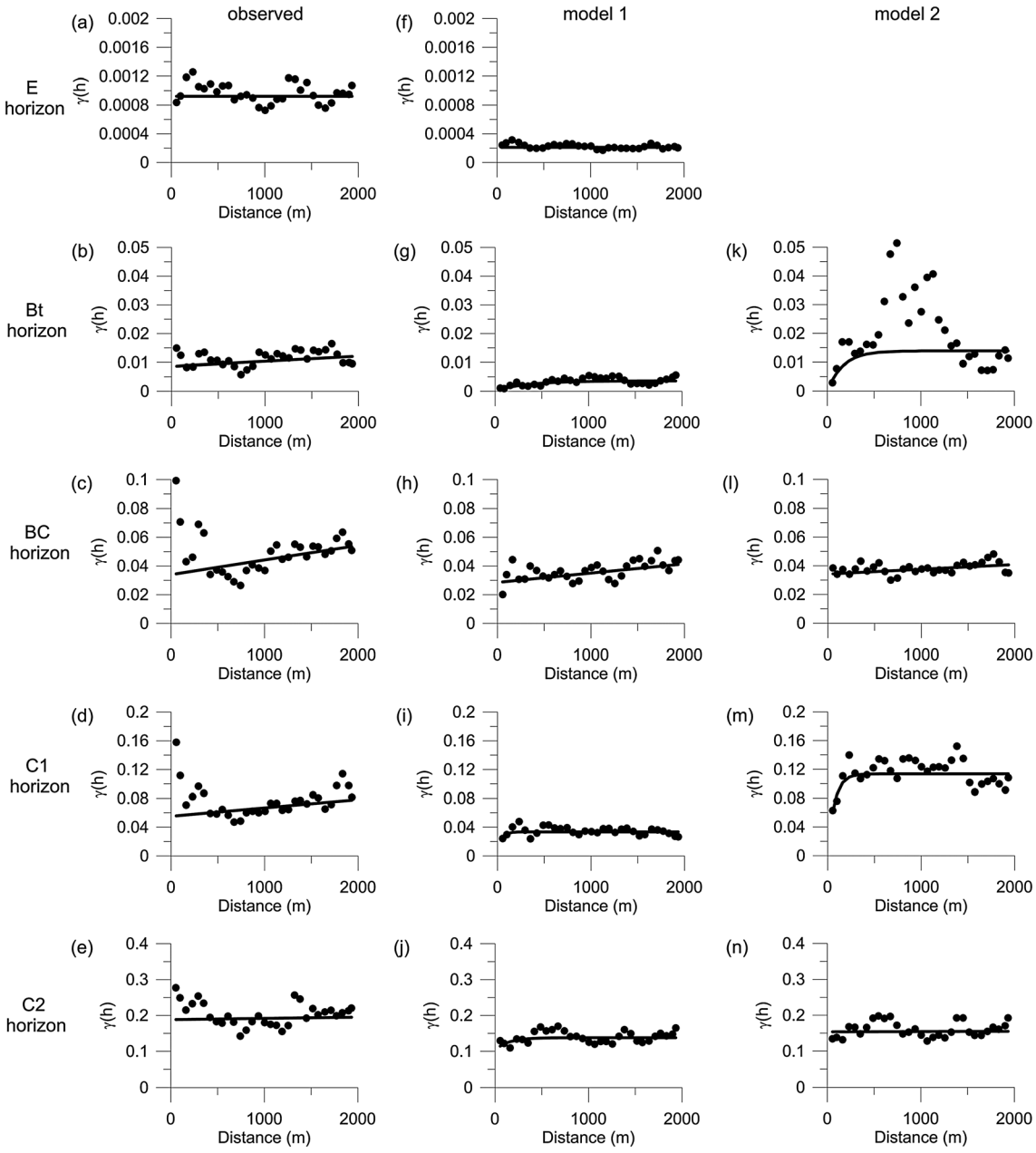

Figure 10. Experimental and fitted semivariograms of the (a–e) observed soil horizon data, (f–j) model 1 without tree uprooting, and (k–n) model 2 including tree uprooting. Note that no E horizon remains at present date (0 B.P.) using model 2.

is larger than the assumed disturbance cycle of 1730 years because the forest vegetation period was discontinuous (Figure 2), and the protocol assumes that young trees do not uproot, which reduces the period in which tree uprootings can occur.

3.3. Geostatistical Analysis and Comparison to Measured Variability

[45] Figure 9 shows the evolution of a typical soil profile under both models, without and with treefalls. With model 1, a full profile that includes all horizons from A to C2 is formed after approximately 5000 years. With model 2, the first treefall at this site occurs after approximately 2000 years (13,000 years B.P.). It can be seen how this event mixes all horizons developed at that time. For a short period, the upper 80 cm classifies into an A horizon according to the protocol. In this example, most of the treefalls occur towards the end of the simulation (0–5000 years B.P.). Because the lower soil horizons (BC-C1-C2) are then already located below the influence depth of the treefalls, these events no longer cause a full mixing of the soil profile. Nevertheless, the mixing of the upper soil layers still results in the disappearance of the E horizon under the classification scheme adopted.

[46] The original data set by *Vanwalleghem et al*. [2010] showed a very weak correlation between the depth of the different soil horizons and landscape attributes. In particular, for the top horizons, E and Bt, no statistically significant relation could be detected. We selected a subset of 108 profiles out of the 399 profiles from the original data set published by

Vanwalleghem et al. [2010], and this led to a slightly different soil-landscape model identified by regression kriging compared to the one reported by *Vanwalleghem et al*. [2010]. In addition, in this study the variable loess cover thickness was included in the analysis because it was hypothesized that this might have an influence on the simulated soil horizon thickness. However, the main conclusion that was drawn based on the original data set that the relation between soil horizon depth and landscape position was weak still holds. As shown in Table 2, for the subset selected in this study, only for the E and C1 horizons, a weak relation was found with wetness index, loess thickness, and soil type: r^2 values for the simple linear regression are all below 0.03. Adjusted r^2 values of the multiple regression model are between 0.04 (BT) and 0.19 (C1). These values are similar to the low explanatory power of the original data set ($n = 300$), with adjusted r^2 values between 0.09 and 0.14. The analysis of the experimental semivariograms (Figure 10) shows that the spatial correlation of the observational data set is low to absent (Figures 10a to 10e). All variograms are characterized by a very high to a pure nugget effect, such as, for example, the E horizon in Figure 10a. The nugget effect is defined as the value of the fitted variogram at distance 0 [*Goovaerts*, 1997]. This high nugget effect shows that there is important soil horizon depth variation at the detailed (10 m) scale.

[47] In contrast to the observed data, the simulated soil horizons by model 1 exhibit a strong correlation with landscape attributes. In this model that simulates soil formation without disturbance by tree throws, all soil horizons are significantly related to at least one landscape variable and for all cases, a significant multiple linear regression model could be established (Table 2). The simulated soil horizon depths correlate with the landscape variables slope angle, wetness index, loess thickness, and soil type. The overall prediction capacity of the soil-landscape model is high for the deeper soil horizons, BC, C1, and C2, and explains between 49% (C2) and 73% (BC) of the variance. For the superficial horizons, E and BT, the model performance is still relatively high and explains between 38% (E) and 53% (BT) of the variance. Analysis of the spatial structure of the regression residuals in the data shows a separation of the horizons in two groups. The deeper soil horizons, BC, C1, and C2, are again characterized by an important nugget effect, showing a nearly complete lack of spatial dependence (Figure 10h to 10j). The superficial horizons on the other hand are characterized by a sill that is a factor two to three lower than the observed data. The sill is defined as the maximal semivariance of the fitted variogram [*Goovaerts*, 1997]. This low sill shows that model 1 underestimates the spatial variation in the data. In addition, the Bt horizon (Figure 10g) does exhibit an increase in semivariance with lag distance.

[48] Finally, the correlation with landscape parameters for model 2, which takes into account treefalls during soil formation, is lower than that for model 1, although it is still higher compared to the observed data (Table 2). Note that with model 2, no E horizon remains at 0 B.P. as the parameters used by the algorithm for horizon classification, and specified under paragraph 2.5, were not met (Figure 9). Therefore, for the superficial soil horizons, we can only use the Bt horizon for comparison. In contrast with model 1 without disturbance, no significant correlation between Bt horizon depth and landscape parameters was found. For the observed data, the multiple linear regression model had a very low predictive power of only 4% of the variability. This means that for this superficial horizon, model 2 actually predicts a situation similar to the one observed in the field. On the other hand, for the deeper soil horizons BC to C2, soil horizons simulated by model 2 did still exhibit a relation to landscape parameters. While the number of significant relations for the simple linear regression model dropped from 14 under model 1 to 8 under model 2, the overall multiple linear regression model showed a significant relation. The predictive power was in the order of that of model 1, explaining between 44% and 71% of the variance. Slope aspect appears to show a stronger relation to the depths of deeper horizons. Wetness index and loess thickness appear to play a less prominent role than with model 1 (Table 2). This corresponds better with the patterns observed in the field. Again, the experimental semivariograms of all soil horizons have a high nugget-to-sill ratio (Figure 10k–10n). However, model 2 does represent the spatial variability in the data more accurately as compared to model 1. For all soil horizons, the sill is close to that of the observed data.

4. Discussion

[49] A process model SoilGen was used to model change in soil properties over the last 15,000 years for 108 locations in a loess parent material. Two scenarios were simulated to assess the effect of treefalls on horizon depths. The horizon classification algorithm allowed us to convert quantitative modeled soil properties (OC, clay content, a clay dispersion indicator, and calcite content) into soil horizon depths. Traditionally, as soil surveys split up the soil profile in diagnostic horizons, much of the available soil data is of a discontinuous nature. While the fitting of a continuous soil depth function from discrete soil horizon data has received considerable attention [*Malone et al*., 2009], the inverse problem has not. The approach proposed here allows us for the first time to explicitly and quantitatively validate our model results with such field data. A calibration to field observations was done to mimic the horizon classification by a soil surveyor. This calibration yielded satisfactory results, but it should be noted that the tuned algorithms are only valid for the test area.

[50] The uprooting model provides acceptable results. The modeled average disturbance cycle of 1890 years is in good agreement with uprooting frequencies found in literature. *Phillips and Marion* [2004] report a mean uprooting cycle for North American forests between 1000 and 2000 years. *Schaetzl and Follmer* [1990] dated tree mounds in Wisconsin and Michigan that were stable somewhat longer, up to 2420 years. In Russia, lower values between 630 and 1000 years have been found (Vasenev and Targul'yan, 1995, cited by *Phillips and Marion* [2004]). The sensitivity of modeled horizon thickness to choices made in the uprooting model was not the subject of the study because of the large runtime of the model. We think that the sensitivity to the disturbance cycle will be relatively small, as the number of treefalls during the simulation period is on average fairly high (Figure 8) and only a few treefalls are necessary to mix topsoil horizons (Figure 9). The effect of wind exposition in the current study was relatively limited as indicated by the values of totalWE (Figure 7) between 0.8 and 1.2 but might have been larger in landscapes with more relief. Probably, the most

sensitive factor was the magnitude and depth of the turbation due to a treefall, which is illustrated by the disappearance of the E horizon in our simulations (Figure 9). We probably overestimated the degree of mixing and the affected depth by treefalls.

[51] More quantitative research is therefore urgently needed on the importance of bioturbation on soil formation. Large uncertainties are associated with the depth and area affected by single treefalls and with the effect of exposure on uprooting probability. In Belgian loess-derived soils, for example, natural soil profiles have been shown to develop a fragipan at the top of the Bt horizon [*Van Vliet and Langohr*, 1982]. Once formed, such a layer would typically affect the soil depth affected by treefalls, as it impedes deep root penetration. It is therefore possible that the constant value of 80 cm for the uprooting depth, as applied in this study, is an overestimation. Also, a time-dependent evolution of the uprooting depth would probably be more realistic, as the evolving soil properties themselves will feed back on the soil depth affected by treefalls. However, at present, no further data is available to justify such an approach.

[52] Previous model studies like, for example, *Gabet and Mudd* [2010] suggested a prominent effect of biomechanical breaking of rocks on total soil depth. As an analogue to our situation, with soils formed on calcareous loess, we could expect to see an effect of treefalls on the total soil profile thickness. However, mixing of calcareous loess within the upper soil profile by bioturbation did not cause any long-term differences in the decalcification depth when comparing the two model scenarios. During the initial phase of the simulation (between 13,000 and 12,000 B.P.), when the decalcification border is still above the uprooting depth, there is a short phase where an uprooting event causes clear differences between models 1 and 2 (Figure 9). However, this effect quickly disappears. The main reason is probably that in this study, soils are relatively deep with respect to the uprooting depth. In shallow soils formed on bedrock, such as in the *Gabet and Mudd* [2010] model, uprooting events will affect the whole soil profile throughout the entire model run.

[53] The results do show clearly that including treefalls in the simulation of soil formation has an important effect on the spatial organization of soil profiles in the landscape. Although none of the models reproduces the observed data, which was expected because treefalls were generated via a stochastic process and initial soil properties were assumed uniform across the landscape, it is clear from Table 2 and Figure 9 that including tree uprooting (model 2) improves the predictions. Especially for the more superficial horizons, model 2 exhibits the same trends as the observed data. The correlation with landscape variables for the Bt horizon disappears as a result of the homogenizing effect of treefalls, as is observed in the field. In contrast, the simple soil formation model (model 1) exhibits a strong correlation with landscape parameters for all soil horizons, which is not observed in the field. However, model 2 also shows some correlation with landscape variables for the deeper soil horizons while this is not observed in the field data set in Table 2. Possible reasons for deviations between model and field estimates of horizon depths may be the following: (i) The assumption of uniform initial properties of the loess cover was not valid; (ii) Variations in soil microrelief as possible remainders from pit-and-mound topography will influence depth estimates of all soil horizons but were not part of the simulations; (iii) Pit-and-mound topography will alter soil water fluxes which are not considered in this model; (iv) Field-estimated horizon depths may be not without error because of the augering technique (non-perfect vertical precision) and of uncertainties in the field classification. Local heterogeneity of parent material properties was identified by *Phillips and Marion* [2005] as a cause of soil diversity. Various authors [*Schaetzl and Follmer*, 1990; *Embleton-Hamann*, 2004] have indicated the importance of pit-and-mound topography on local soil genesis; thus, these issues need more study. The first two reasons could be the subject of future simulation studies, as the SoilGen model can be run with nonhomogeneous parent materials and also with additions or losses of topsoil. Each simulated scenario took 1940 CPU days (1 core), equivalent to 4 months of computing on four quad-core computers simultaneously. This large computational demand limited the number of simulated scenarios.

[54] Given the fact that model 1 is fully deterministic and the only factors that determine differences in soil formation are slope angle, slope aspect, and thickness of the loess cover, it is surprising that terrain attributes and thickness of loess cover do not fully represent resulting soil horizon variability. Apparently, some effective covariates are missing, or there is some noise in the DEM due to measurement errors, or the regression kriging method fails to detect (possibly nonlinear) relations between covariates and horizon thicknesses. It may be worthwhile to try out other DSM methods with the current data set to identify their potential in case that the soil-landscape relation is arguably deterministic as in model 1.

5. Conclusions

[55] A key challenge in the quantitative modeling of soil formation is to include the effect of bioturbation. While in agricultural areas, the spatial pattern of soil properties is largely controlled by soil erosion and redistribution, in natural areas previous work showed that bioturbation by tree uprooting has a large effect on the spatial organization of soil profile depth. We present here the first model that includes this effect in soil evolution. We developed a conversion protocol between simulated soil properties and soil horizon codes and calibrated to field estimates.

[56] A model that generates treefall events as a function of annual distributions of wind direction and wind speed was developed, using a DEM and an average disturbance cycle by treefalls.

[57] Application of a process-based simulation model for soil genesis with spatially varying slope angle, slope aspect, and loess cover thickness resulted in a spatial distribution of horizon depths that could reasonably well be modeled by a regression kriging approach; however, regression kriging was not able to detect and model all soil variation, even while it was fully deterministically linked to slope angle and its aspect.

[58] Application of this model run with simulated treefalls resulted in a spatial distribution of horizon depths that could not well be modeled by a regression kriging approach. As this was also found in the field data, the occurrence of treefalls could be an explanation of the lack of spatial structure. In deeper parts of the soil profile, spatial patterns of horizon depths were still well detectable (contrasting to field observations), which may be explained by variations in parent material properties, microrelief, and random errors in field estimates.

[59] **Acknowledgments.** Tom Vanwalleghem acknowledges funding by the Spanish Ministry of Economy and Competitiveness (through the Fellowship Ramón y Cajal RYC-2010-07166 and the research project AGL2012-40128-C03-02). Emmanuel Opolot acknowledges funding from the Belgian Science Policy Office (project BELSPO/IUAP p7/24).

References

Armson, K. A., and R. J. Fessenden (1973), Forest windthrows and their influence on soil morphology, *Soil Sci. Soc. Am. Proc.*, *37*, 781–783.

Beke, G. J., and J. A. McKeague (1984), Influence of tree windthrow on the properties and classification of selected forested soils from Nova Scotia, *Can. J. Soil Sci.*, *64*, 195–207.

Beven, K. J., and M. J. Kirkby (1979), A physically based variable contributing area model of basin hydrology, *Hydrol. Sci. Bull.*, *24*(1–3), 43–69.

Chaplot, V., B. Bouahom, and C. Valentin (2009), Soil organic carbon stocks in Laos: Spatial variations and controlling factors, *Global Change Biol.*, *16*, 1380–1393.

Claessens, L., A. Knapen, M. G. Kitutu, J. Poesen, and J. A. Deckers (2007), Modelling landslide hazard, soil redistribution and sediment yield of landslides on the Ugandan footslopes of Mount Elgon, *Geomorphology*, *90*(1–2), 23–35, doi:10.1016/j.geomorph.2007.01.007.

Coleman, K., and D. S. Jenkinson (2005), RothC-26.3 A Model for the turnover of carbon in soil, November 1999 issue, modified April 2005. [Available at http://www.rothamsted.bbsrc.ac.uk/aen/carbon/download.htm].

Davis, B. A. S., S. Brewer, A. C. Stevenson, J. Guiot, and Data Contributors (2003), The temperature of Europe during the Holocene reconstructed from pollen data, *Quat. Sci. Rev.*, *22*, 1701–1716.

De Keersmaeker, L., H. Baeté, B. Christiaens, M. Esprit, P. Van de Kerckhove, and K. Vandekerkhove (2009), Bosreservaat Pruikenmakers (Meerdaalwoud): monitoringrapport. Monitoring van de dendrometrische gegevens en de vegetatie in steekproefcirkels en een kernvlakte, Rapporten van het Instituut voor Natuur- en Bosonderzoek 2009 (11), Instituut voor Natuur- en Bosonderzoek, Brussel.

De Vries, W., and M. Posch (2003), *Derivation of Cation Exchange Constants for Sand, Loess, Clay and Peat Soils on the Basis of Field Measurements in the Netherlands*, Alterra-Report 701, 50 pp., Alterra Green World Research, Wageningen.

Dlugoß, V., P. Fiener, and K. Schneider (2010), Layer-specific analysis and spatial prediction of soil organic carbon using terrain attributes and erosion modeling, *Soil Sci. Soc. Am. J.*, *74*(3), 922–935.

Embleton-Hamann, C. (2004), Processes responsible for the development of a pit and mound microrelief, *Catena*, *57*(2), 175–188.

Erpul, G., D. Gabriels, W. M. Cornelis, N. H. Samray, and T. Guzelordu (2008), Sand detachment under rains with varying angle of incidence, *Catena*, *72*, 413–422.

Food and Agriculture Organization (FAO) (2006), *Guidelines for Soil Description*, 4th ed., FAO, Rome.

Finke, P. A. (2012), Modeling the genesis of Luvisols as a function of topographic position in loess parent material, *Quat. Int.*, *265*, 3–17.

Finke, P. A., and W. J. P. Bosma (1993), Obtaining basic simulation data for a heterogeneous field with stratified marine soils, *Hydrol. Processes*, *7*, 63–75.

Finke, P. A., and J. L. Hutson (2008), Modelling soil genesis in calcareous löss, *Geoderma*, *145*, 462–479.

Gabet, E. J., and S. M. Mudd (2010), Bedrock erosion by root fracture and tree throw: A coupled biogeomorphic model to explore the humped soil production function and the persistence of hillslope soils, *J. Geophys. Res.*, *115*, F04005, doi:10.1029/2009JF001526.

Gabet, E., O. J. Reichmann, and E. W. Seabloom (2003), The effects of bioturbation on soil processes and sediment transport, *Annu. Rev. Earth Planet. Sci.*, *31*, 249–273.

Gessler, P. E., O. A. Chadwick, F. Chamron, K. Holmes, and L. Althouse (2000), Modeling soil–landscape and ecosystem properties using terrain attributes, *Soil Sci. Soc. Am. J.*, *64*, 2046–2056.

Godefroid, S., and N. Koedam (2010), Tree-induced soil compaction in forest ecosystems: Myth or reality?, *Eur. J. For. Res.*, *129*, 209–217.

Goovaerts, P. (1997), *Geostatistics for Natural Resources Evaluation*, Oxford Univ. Press, New York.

Gullentops, F. (1954), Contribution a la chronologie du Pléistocène et des formes de rélief en Belgique, *Mém. Inst. Géol. Univ. Louvain*, *18*, 123–252.

Hancock, G. R., K. G. Evans, J. McDonnell, and L. Hopp (2012), Ecohydrological controls on soil erosion and landscape evolution, *Ecohydrology*, *5*(4), 478–490, doi:10.1002/eco.241.

Hargreaves, G. H., and Z. A. Samani (1985), Reference crop evapotranspiration from temperature, *Appl. Eng. Agric.*, *1*(2), 96–99.

Horwath, J. L., and D. L. Johnson (2006), Mima-type mounds in southwest Missouri: Expressions of 220 point-centered and locally thickened biomantles, *Geomorphology*, *77*(3–4), 308–319.

Hutson, J. L. (2003), *LEACHM: A Process-Based Model of Water and Solute Movement, Transformations, Plant Uptake and Chemical Reactions in the Unsaturated Zone. Version 4*, Research Series No R03-1, Dept. of Crop and Soil Sciences, Cornell University, Ithaca, N.Y.

International Union of Soil Science Working Group WRB (2006), World Reference Base for Soil Resources 2006, World Soil Resources Reports No. 103, 2nd ed., FAO, Rome.

Johnson, D. L., J. E. J. Domier, and D. N. Johnson (2005), Reflections on the nature of soil and its biomantle, *Ann. Assoc. Am. Geogr.*, *95*(1), 11–31.

Kaste, J. M., A. M. Heimsath, and B. C. Bostick (2007), Short-term soil mixing quantified with fallout radionuclides, *Geology*, *35*(3), 243–246.

Kowalinski, S., L. J. Pons, and S. Slager (1972), Micromorphological comparison of three soils derived from loess in different climatic regions, *Geoderma*, *7*, 141–158.

Langohr, R. (1993), Types of tree windthrow, their impact on the environment and their importance for the understanding of archaeological excavation data, *Helinium*, *XXXIII*(1), 36–49.

Li, Y., and M. J. Lindstrom (2001), Evaluating soil quality–soil redistribution relationship on terraces and steep hillslope, *Soil Sci. Soc. Am. J.*, *65*, 1500–1508.

Lutz, H. J., and F. S. Griswold (1939), The influence of tree roots on soil morphology, *Am. J. Sci.*, *237*(6), 389–400.

Lyles, L., L. A. Disrud, and N. P. Woodruff (1969), Effects of soil physical properties, rainfall characteristics and wind velocity on clod disintegration by simulated rainfall, *Soil Sci. Am. Proc.*, *33*, 302–306.

Malone, B. P., A. B. McBratney, B. Minasny, and G. M. Laslett (2009), Mapping continuous depth functions of soil carbon storage and available water capacity, *Geoderma*, *154*(1–2), 138–152.

Mauersberger, F. (2001), Modellrechnungen zum Einfluss des Aufprallwinkels der Regentropfen auf die Mobilisierung und den Transport von Bodenpartikeln, Diploma thesis, Technical University Freiburg.

Maxwell, S., D. S. Green, and W. Zhang (2010), Identifying the determinants of windthrow damage in wildlife tree patches in the Boreal White and Black Spruce biogeoclimatic zone of northeastern British Columbia, *J. Ecosyst. Manage.*, *10*(3), 1–8.

McBratney, A. B., M. L. Mendonça Santos, and B. Minasny (2003), On digital soil mapping, *Geoderma*, *117*, 3–52.

Moore, I., P. Gessler, G. Nielsen, and G. Peterson (1993), Soil attribute prediction using terrain analysis, *Soil Sci. Soc. Am. J.*, *57*, 443–452.

Mücher, H. J. (1973), Enkele aspecten van de loess en zijn noordelijke begrenzing, in het bijzonder in Belgisch en Nederlands Limburg en het daaraangrenzende gebied in Duitsland, *K.N.A.G. Geogr. Tijdschr.*, *VII*(4), 259–276.

Odeh, I. O. A., A. B. McBratney, and D. J. Chittleborough (1994), Spatial prediction of soil properties from landform attributes derived from a digital terrain model, *Geoderma*, *63*, 197–214.

Phillips, J. D. (2007), Formation of texture contrast soils by a combination of bioturbation and translocation, *Catena*, *70*, 92–104.

Phillips, J. D. (2008), Soil system modelling and generation of field hypotheses, *Geoderma*, *145*(3–4), 419–425.

Phillips, J. D., and D. A. Marion (2004), Pedological memory in forest soil development, *For. Ecol. Manage.*, *188*, 363–380.

Phillips, J. D., and D. A. Marion (2005), Biomechanical effects, lithological variations, and local pedodiversity in some forest soils of Arkansas, *Geoderma*, *124*, 73–89.

Poesen, J., B. van Wesemael, G. Govers, J. Martinez-Fernandez, P. Desmet, K. Vandaele, T. Quine, and G. Degraer (1997), Patterns of rock fragment cover generated by tillage erosion, *Geomorphology*, *18*(3–4), 183–197.

Pye, K. (1983), Grain surface textures and carbonate content of Late Pleistocene loess from West Germany and Poland, *J. Sediment. Petrol.*, *53*(3), 973–980.

Rantakari, M., A. Lehtonen, T. Linkosalo, M. Tuomi, P. Tamminen, J. Heikkinen, J. Liski, R. Makipaa, H. Ilvesniemi, and R. Sievanen (2012), The Yasso07 soil carbon model: Testing against repeated soil carbon inventory, *For. Ecol. Manage.*, *286*, 137–147, doi:10.1016/j.foreco.2012.08.041.

Šamonil, P., K. Král, and L. Hort (2010), The role of tree uprooting in soil formation: A critical literature review, *Geoderma*, *157*, 65–79.

Šamonil, P., M. Vaitera, S. Bek, B. Sebkova, T. Vrska, and J. Houska (2011), Soil variability through spatial scales in a permanently disturbed natural spruce-fir-beech forest, *Eur. J. For. Res.*, *130*, 1075–1092.

Sauer, D., P. A. Finke, I. Schülli-Maurer, R. Sperstad, R. Sørensen, H. I. Høeg, and K. Stahr (2012), Testing a soil development model against southern Norway soil chronosequences, *Quat. Int.*, *265*, 18–31.

Schaetzl, R. J., and L. Follmer (1990), Longevity of treethrow microtopography: Implications for mass wasting, *Geomorphology*, *3*(2), 113–123.

Schaetzl, R. J., D. L. Johnson, S. F. Burns, and T. W. Small (1989), Tree uprooting: Review of terminology, process, and environmental implications, *Can. J. For. Res.*, *19*, 1–11.

Schmidt, J. (1992), Modelling long-term soil loss and landform change, in *Overland Flow—Hydraulics and Erosion Mechanics*, edited by A. J.

Abrahams and A. D. Parsons, pp. 389–413, University College London Press, London.

Swift, L. W., Jr. (1976), Algorithm for solar radiation on mountain slopes, *Water Resour. Res.*, *12*(1), 108–112, doi:10.1029/WR012i001p00108.

Tesfa, T. K., D. G. Tarboton, D. G. Chandler, and J. P. McNamara (2009), Modeling soil depth from topographic and land cover attributes, *Water Resour. Res.*, *45*, W10438, doi:10.1029/2008WR007474.

Ulanova, N. G. (2000), The effects of windthrow on forests at different spatial scales a review, *For. Ecol. Manage.*, *135*, 155–167.

Van Vliet-Lanoë, B., and R. Langohr (1982), Evidence of disturbance by frost of pore ferriargilans in silty soils of Belgium and Northern France, in *Soil Micromorphology*, edited by P. Bullock and C. Murphy, pp. 511–518, ABA publ., London.

Vanwalleghem, T., M. Van Den Eeckhaut, J. Poesen, J. Deckers, J. Nachtergaele, K. Van Oost, and C. Slenters (2003), Characteristics and controlling factors of old gullies under forest in a temperate humid climate: A case study from the Meerdaal Forest (Central Belgium), *Geomorphology*, *56*, 15–29.

Vanwalleghem, T., J. Poesen, M. Van Den Eeckhaut, J. Nachtergaele, and J. Deckers (2005), Reconstructing rainfall and land use conditions leading to the development of old gullies, *Holocene*, *15*, 378–386.

Vanwalleghem, T., H. R. Bork, J. Poesen, M. Dotterweich, G. Schmidtchen, J. Deckers, S. Scheers, and M. Martens (2006), Prehistoric and Roman gullying in the European loess belt: A case study from central Belgium, *Holocene*, *16*(3), 393–401.

Vanwalleghem, T., J. Poesen, A. McBratney, and J. Deckers (2010), Spatial variability of soil horizon depth in natural loess-derived soils, *Geoderma*, *157*, 37–45.

Verbruggen, C., L. Denys, and P. Kiden (1996), Belgium, in *Palaeoecological Events During the Last 15000 Years. Regional Syntheses of Palaeoecological Studies of Lakes and Mires in Europe*, edited by B. E. Berglund et al., pp. 453–474, John Wiley, Chistester.

Wallach, D., S. Buis, P. Lecharpentier, J. Bourges, P. Clastre, M. Launay, J. E. Bergez, M. Guerif, J. Soudais, and E. Justes (2011), A package of parameter estimation methods and implementation for the STICS crop-soil model, *Environ. Modell. Software*, *26*(4), 386–394, doi:10.1016/j.envsoft.2010.09.004.

Webster, R., and M. A. Oliver (1992), Sample adequately to estimate variograms of soil properties, *J. Soil Sci.*, *43*(1), 177–192.

Whelan, B. M., A. B. McBratney, and B. Minasny (2001), Vesper – Spatial prediction software for precision agriculture, in *ECPA 2001. Third European Conference on Precision Agriculture*, edited by G. Grenier and S. Blackmore, pp. 139–144, Agro Montpellier, Ecole Nationale Agronomique de Montpellier, Montpellier.

Wintle, A. G., and K. Brunnacker (1982), Ages of volcanic tuff in Rhein-Hessen obtained by thermo-luminescence dating of loess, *Naturwissenschaften*, *69*, 181–183.

Yoo, K., J. Ji, A. Aufdenkampe, and J. Klaminder (2011), Rates of soil mixing and associated carbon fluxes in a forest versus tilled agricultural field: Implications for modeling the soil carbon cycle, *J. Geophys. Res.*, *116*, G01014, doi:10.1029/2010JG001304.

Yu, Y., P. A. Finke, Z. T. Guo, and H. Wu (2012), Sensitivity analysis and calibration of a soil carbon model (SoilGen2) in two contrasting loess forest soils, *Geosci. Model Dev. Discuss.*, *5*, 1817–1849. [Available at http://www.geosci-model-dev-discuss.net/5/1817/2012/gmdd-5-1817-2012.html].